Journal of Thermal Analysis and Calorimetry (2019) 135:1629–1641
https://doi.org/10.1007/s10973-018-7517-z

Analytical investigation of nanoparticle migration in a duct considering thermal radiation

Zhixiong Li[1,2] · S. Saleem[3] · Ahmad Shafee[4] · Ali J. Chamkha[5,6] · Sunwen Du[7]

Received: 24 May 2018 / Accepted: 28 June 2018 / Published online: 21 July 2018

Abstract

Buongiorno model is applied to investigate nanofluid migration through a permeable duct in the presence of external forces. Influences of radiation and Joule heating on first law equation are added. Final formulas are solved via differential transform method. Roles of suction, thermophoretic, radiation and Brownian motion parameters, Schmidt number, Hartmann number, Eckert number were presented. Results show that temperature gradient improves with the enhancement of Reynolds number, suction and Radiation parameters. *Nu* augments with the augmentation of Hartmann and Eckert numbers, while reverse behavior is seen for skin friction coefficient. Also, it can be concluded that Nusselt number enhances with the increase in radiation parameter but it decreases with the increase in Brownian motion.

Keywords Differential transform method · Porous duct · Nanoparticle · Lorentz forces · Buongiorno model

List of symbols

B_0 Magnetic induction (Tesla)
Pr Prandtl number
Rd Radiation parameter
Ha Hartmann number
C_p Specific heat capacity (J/kgK)
v, u Vertical and horizontal velocities (m/s)
q_r Thermal radiation (W)
T Fluid temperature (K)

Greek symbols

σ_e Stefan–Boltzmann constant
μ Dynamic viscosity (Pa s)
ϕ Volume fraction of nanofluid
α Thermal diffusivity ($m^2\ s^{-1}$)
η Similarity-independent variable
β_R Mean absorption coefficient
σ Electrical conductivity

Subscripts

T Thermal quantity
f Base fluid

✉ Zhixiong Li
zhixiongli@cumt.edu.cn

1 School of Engineering, Ocean University of China, Qingdao 266110, China

2 School of Mechanical, Materials, Mechatronic and Biomedical Engineering, University of Wollongong, Wollongong, NSW 2522, Australia

3 Department of Mathematics, College of Science, King Khalid University, Abha 61413, Saudi Arabia

4 Public Authority of Applied Education & Training, College of Technological Studies, Applied Science Department, Shuwaikh, Kuwait

5 Mechanical Engineering Department, Prince Sultan Endowment for Energy and Environment, Prince Mohammad Bin Fahd University, Al-Khobar 31952, Saudi Arabia

6 RAK Research and Innovation Center, American University of Ras Al Khaimah, Ras Al Khaimah, United Arab Emirates

7 College of Mining Technology, Taiyuan University of Technology, Yingze West St. 79, Taiyuan 030024, P. R. China

Introduction

Nanoscience can suggest applicable working fluid to improve thermal behavior. Karimipour et al. [1] investigated the impact of kind of nanoparticles on nanofluid MHD flow in a microchannel. Maleki et al. [2] simulated non-Newtonian nanofluid flow over a permeable plate. Sheikholeslami et al. [3] presented an experimental study to analyze exergy loss during condensation process. Hosseini et al. [4] offered the new method for estimating thermal conductivity of nanofluids. They used interfacial

shell-dependent dimensionless model. Esfahani et al. [5] investigated oil-based nanofluid transportation. They compared numerical result with experimental data. Sheikholeslami and Rokni [6] published a report for application ferrofluid. Comprehensive review paper has been published by Sheikholeslami and Ganji [7] to show importance of nanotechnology. Haq et al. [8] investigated carbon nanotube pulsatile flow due to magnetic forces in an annulus. Sheikholeslami [9] utilized nanoparticle-enhanced PCM for discharging process. He simulated this unsteady problem with FEM. Arani et al. [10] studied the heat transfer of carbon nanotubes (SWCNT) nanofluid in a heat sink.

Sheikholeslami et al. [11] simulated second law analysis of nanofluid forced convection in a heat exchanger. Khodabandeh et al. [12] investigated nanofluid flow in a horizontal spiral coil. This geometry can be used for solar ponds. Tao and He [13] presented the NEPCM charging process in an energy storage system. Ahmed et al. [14] reported time-dependent flow along a heated plate. Sheikholeslami et al. [15] investigated discharging process of NEPCM in the presence of thermal radiation. Alrashed et al. [16] presented a regression for characteristics of carbon-based nanofluid. Jafaryar et al. [17] investigated turbulent heat transfer in a pipe equipped with twisted tape. Nasiri et al. [18] utilized SPH for nanofluid flow over a cylinder. Sheikholeslami [19] employed magnetic field to expedite the solidification process. Goodarzi et al. [20] investigated two-phase flow of nanofluid in a cavity with lid wall. Sheikholeslami et al. [21] investigated three-dimensional MHD flow of nanofluid in a cubic cavity. They used mesoscopic approach. Selecting effective working fluid becomes hot topics in recent years [22–75].

In this paper, radiation of nanofluid through a permeable duct is investigated using DTM. Impacts of suction, radiation, Brownian motion and thermophoretic parameters, Schmidt and Hartmann, Eckert numbers have been presented.

Governing equation

Steady two-phase flow of nanofluid in a semipermeable duct is considered. Figure 1 shows the geometry and boundary conditions. Constant vertical magnetic field effect has been applied. Effects of Joule heating and radiation on temperature distribution are employed. The lower surface is hot, and the upper one is cold. Governing formulas are [22]:

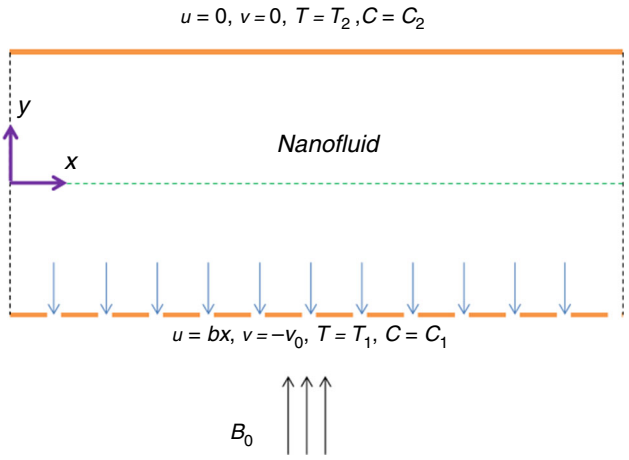

Fig. 1 Geometry of the problem

$$\frac{\partial v}{\partial y}+\frac{\partial u}{\partial x}=0 \tag{1}$$

$$\rho_{\mathrm{f}}\left(v\frac{\partial u}{\partial y}+u\frac{\partial u}{\partial x}\right)=\mu\left(\frac{\partial^2 u}{\partial y^2}\right)-\frac{\partial p}{\partial x}-\sigma B_0^2 u, \tag{2}$$

$$\rho_{\mathrm{f}}\left(v\frac{\partial v}{\partial y}+\frac{\partial v}{\partial x}u\right)=-\frac{\partial p}{\partial y}+\mu\left(\frac{\partial^2 v}{\partial x^2}\right) \tag{3}$$

$$\begin{aligned}\left(u\frac{\partial T}{\partial x}+v\frac{\partial T}{\partial y}\right)(\rho C_{\mathrm{p}})_f &= k\left(\frac{\partial^2 T}{\partial y^2}\right)\\ &\quad+(\rho C_{\mathrm{p}})_{\mathrm{p}}\left[D_B\left\{\frac{\mathrm{d}C}{\mathrm{d}y}.\frac{\mathrm{d}T}{\mathrm{d}y}\right\}\right.\\ &\quad\left.+(D_{\mathrm{T}}/T_2)\left\{\left(\frac{\mathrm{d}T}{\mathrm{d}y}\right)^2\right\}\right]\\ &\quad-\frac{\partial q_r}{\partial y}+\sigma B_0^2 u^2,\\ q_r &= -\frac{4\sigma_{\mathrm{e}}}{3\beta_{\mathrm{R}}}\frac{\partial T^4}{\partial y}\end{aligned} \tag{4}$$

$$\frac{\partial C}{\partial y}v+\frac{\partial C}{\partial x}u=\left(\frac{D_T}{T_2}\right)\left\{\frac{\mathrm{d}^2 C}{\mathrm{d}y^2}\right\}+D_{\mathrm{B}}\frac{\partial^2 C}{\partial y^2} \tag{5}$$

where according to [76], $T^4 \cong 4T_{\mathrm{c}}^3 T-3T_{\mathrm{c}}^4$.

Boundary conditions are:

$$\begin{aligned}&\text{at}\quad y=-a \quad C=C_1,\ u=bx,\ v=-v_0,\ T=T_1,\\ &\text{at}\quad y=+a \quad C=C_2,\ v=0,\ u=0,\ T=T_2,\end{aligned} \tag{6}$$

The following definitions are used to convert equations to ODEs [22]:

$$\eta = \frac{y}{a},\ u = bxf'(\eta),\ \ v = -abf(\eta),\ \ \theta = \frac{T - T_1}{T_1 - T_2},\ \phi = \frac{C - C_1}{C_1 - C_2} \tag{7}$$

According to Eq. (7), final ODEs are:

$$f^{iv} + R(f'''f - f''f') - Ha^2 f'' = 0 \tag{8}$$

$$\left(1 + \frac{4}{3}Rd\right)\theta'' + \Pr f\theta' + Ha^2\, Ec\, \frac{\Pr}{R} f'^2 + Nb\theta'\phi' + Nt\theta'^2 = 0 \tag{9}$$

$$\phi'' + Sc(f\phi') + \frac{Nt}{Nb}\theta'' = 0 \tag{10}$$

where $R, Ha, Rd, Ec, \Pr, Nt, Nb, Sc$ are:

$$R = \frac{a^2 b}{\upsilon},\ Ha = B_0\, a\sqrt{\frac{\sigma}{\mu}}, Rd = 4\sigma_e T_c^3/(\beta_R k),$$
$$Ec = \frac{\rho_f (bx)^2}{(\rho C_p)\Delta T}, \Pr = \left(\rho C_p\right)_f \frac{a^2 b}{k},$$
$$Nt = \frac{\Delta T \left(\rho C_p\right)_p D_T}{\left(\rho C_p\right)_f \alpha}, Nb = \Delta C \alpha^{-1} D_B \left(\rho C_p\right)_f^{-1} \left(\rho C_p\right)_p,$$
$$Sc = \frac{\upsilon}{D},$$
$$A_1 = \frac{\rho_{nf}}{\rho_f}, A_2 = \frac{\mu_{nf}}{\mu_f}, A_4 = \frac{k_{nf}}{k_f}, A_3 = \frac{\left(\rho C_p\right)_{nf}}{\left(\rho C_p\right)_f}, A_5 = \frac{\sigma_{nf}}{\sigma_f} \tag{11}$$

Moreover, at $\eta = 1, -1$ we have:

$$\theta(1) = 0,\ \phi(1) = 0,\ f(1) = 0, f(-1) = \frac{v_0}{ab} = \lambda,\ \phi(-1) = 1, f'(-1) = 1,\ f'(1) = 0,\ \theta(-1) = 1 \tag{12}$$

Nu and C_f over the bottom wall are

$$Nu = |\theta'(-1)|, C_f = |f''(-1)| \tag{13}$$

Solution with differential transformation method

The basic idea of DTM exists in [23]. Applying the differential transforms for Eqs. (8–10) gives:

$$\begin{aligned}&(k+3)(k+1)(4+k)(2+k)F[k+4] \\ &\quad - Ha^2 f''(2+k)(k+1)F[2+k] \\ &\quad - R\sum_{m=0}^{k}((2+m)(1+m)F[m+2](k+1-m)F[k+1-m]) \\ &\quad - R\sum_{m=0}^{k}((3+m)(m+1)(2+m)F[3+m]F[-m+k]) = 0\end{aligned} \tag{14}$$

$$F[3] = a_4, F[0] = a_1,\ F[2] = a_3,\ F[1] = a_2, \tag{15}$$

$$\begin{aligned}&(1+k)\left(1+\frac{4}{3}Rd\right)(2+k)\Theta[2+k] \\ &\quad + \Pr\sum_{m=0}^{k}(F[-m+k](1+m)\Theta[1+m]) \\ &\quad + Ha^2\, Ec\, \frac{\Pr}{R}\sum_{m=0}^{k}((1+m)F[-m+k+1](k-m+1)F[1+m]) \\ &\quad + Nb\sum_{m=0}^{k}((-m+k+1)\Theta[1+m](1+m)\Phi[-m+k+1]) \\ &\quad + Nt\sum_{m=0}^{k}(\Theta[1+m](-m+k+1)\Theta[k-m+1](1+m)) = 0\end{aligned} \tag{16}$$

$$\Theta[0] = a_5,\ \ \Theta[1] = a_6 \tag{17}$$

$$\begin{aligned}&(2+k)(1+k)\Phi[1+k+1] + Sc\sum_{m=0}^{k}(F[-m+k]\Phi[m+1](+1+m)) \\ &\quad + (k+2)(1+k)\frac{Nt}{Nb}\Theta[k+2] = 0 \\ &\quad + Ha^2\, Ec\, \frac{\Pr}{R}\sum_{m=0}^{k}((m+1)F[m+1](k-m+1)F[k-m+1]) \\ &\quad + Nb\sum_{m=0}^{k}((m+1)(k-m+1)\Phi[k-m+1]\Theta[m+1]) \\ &\quad + Nt\sum_{m=0}^{k}((-m+k+1)(m+1)\Theta[-m+k+1]\Theta[1+m]) = 0\end{aligned} \tag{18}$$

$$\Phi[0] = a_7,\ \ \Phi[1] = a_8 \tag{19}$$

According to previous equations,

$$\begin{aligned}&F[3] = a_4, F[2] = a_3, F[1] = a_2,\ F[0] = a_1, \\ &F[4] = \frac{1}{12}Ha^2 a_3 + \frac{1}{12}R\, a_2\, a_3 - \frac{1}{4}R\, a_1\, a_4, \\ &F[5] = \frac{1}{20}Ha^2 a_4 + \frac{1}{30}R\, a_3^2 - \frac{1}{60}RHa^2\, a_1\, a_3 \\ &\qquad + \frac{1}{20}(R)^2\, a_1^2 a_4, \ldots\end{aligned} \tag{20}$$

$$\Theta[0] = a_5, \quad \Theta[1] = a_6,$$
$$\Theta[2] = -1.5\frac{1}{R(3+4Rd)}\left(Nt\,R\,a_6^2 + \Pr\, a_1 a_6\, R + Ha^2\, \Pr\, Ec\, a_2^2 + Nb\, a_8 a_6 R\right), \ldots \tag{21}$$

$$\Phi[0] = a_7, \quad \Phi[1] = a_8,$$
$$\Phi[2] = \frac{0.5}{Nb\,R(3+4Rd)}\left(-3Sc\,a_1\,a_8\,Nb\,R - 4Sc\,a_1\,a_8\,Nb\,R\,Rd + 3\,Nt^2\,a_6^2\,R + 3Nt\ \Pr\ a_1\,a_6 R + 3\,Nt\,Nb\,a_6\,a_8 R\right), \ldots \tag{22}$$

Finally, we have:

$$F(\eta) = a_1 + a_2\eta + a_3\eta^2 + a_4\eta^3 + \left(\frac{1}{12}Ha^2 a_3 + \frac{1}{12}R\,a_2\,a_3 - \frac{1}{4}R\,a_1\,a_4\right)\eta^4 + \cdots \tag{23}$$

$$\Theta(\eta) = a_5 + a_6\eta + \left(\frac{-1.5}{\mathrm{R}(3+4Rd)}\left(Nt\,R\,a_6^2 + \Pr\, a_1 a_6\, R + Ha^2\, \Pr\, Ec\, a_2^2 + Nb\, a_8 a_6 R\right)\right)\eta^2 + \cdots \tag{24}$$

$$\Phi(\eta) = a_7 + a_8\eta + \frac{0.5}{Nb\,R(3+4Rd)}\left(-3Sc\,a_1\,a_8\,Nb\,R - 4Sc\,a_1\,a_8\,Nb\,R\,Rd + 3\,Nt^2\,a_6^2\,R + 3Nt\ \Pr\ a_1\,a_6 R + 3\,Nt\,Nb\,a_6\,a_8 R\right)\eta^2 + \cdots \tag{25}$$

So, $a_1, a_2, a_3, a_4, a_5, a_6, a_7, a_8$ can be obtained. By inserting these values into Eqs. (23–25), the expression of $F(\eta), \Theta(\eta)$ and $\Phi(\eta)$ can be obtained which are the transformation of $f(\eta), \theta(\eta)$ and $\phi(\eta)$, respectively.

Results and discussion

Roles of external forces on two-phase flow of CuO–H_2O in a semipermeable duct with stretching wall are investigated. Influence of radiation and Joule heating on first law equation is employed. ODEs are obtained via similarity transformation and solved by differential transform method. Figure 2 illustrates the verifications of presented result with those of obtained in previous works [77,78].

Impact of Reynolds number on f, θ and ϕ is demonstrated in Fig. 3. Vertical velocity and θ profiles decrease with the increase in Re. Horizontal velocity near the

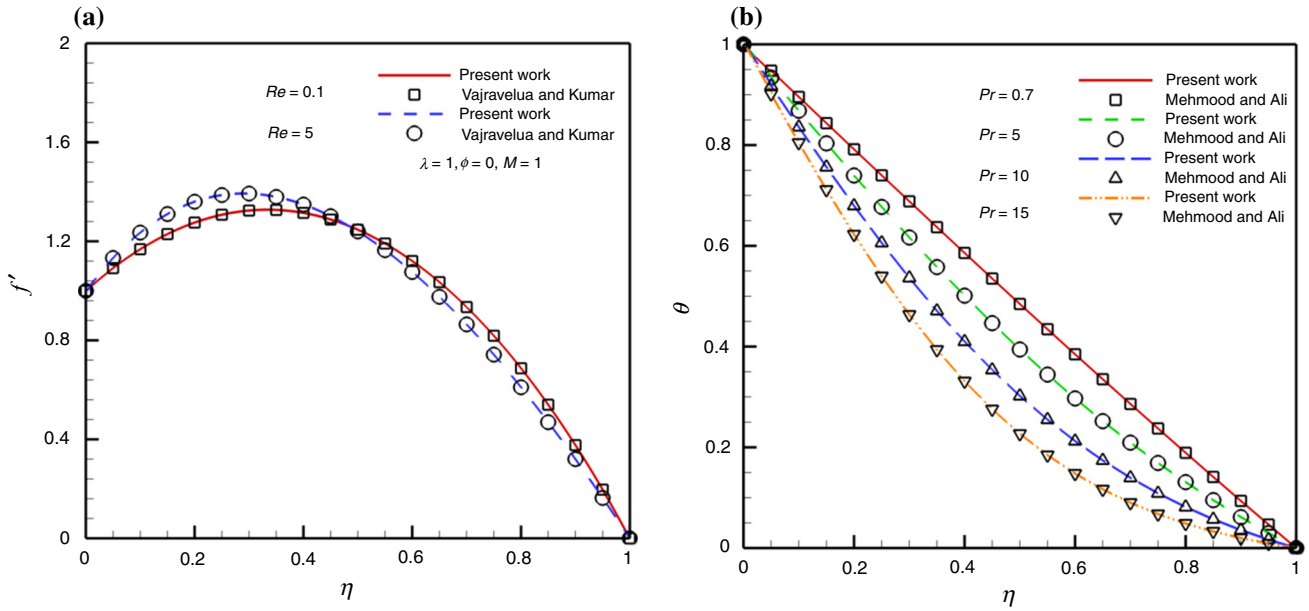

Fig. 2 Comparison of the velocity and temperature profiles between the present work and (**a**) [77]; **b** [78] for different values of *Pr* when $\lambda = 0.5$, $M = 1$, R = 0.5 and $Kr = 0.5$

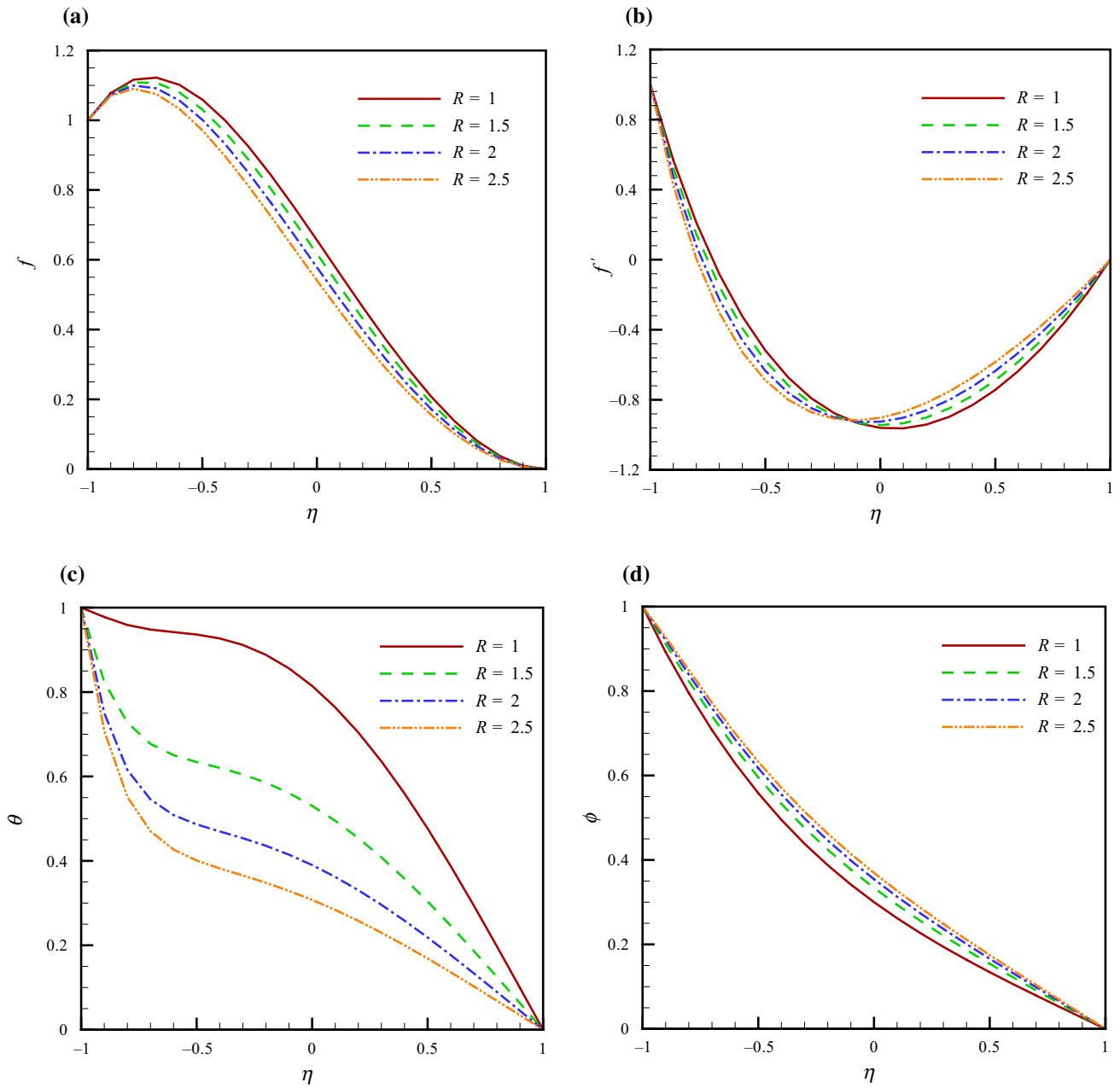

Fig. 3 Effect of Reynolds number on velocity, temperature, concentration profiles when $Ha = 1$, $\lambda = 1, \mathrm{Rd} = 0.5, Ec = 0.5$, $Sc = 1$, $Nt = 0.001, Nb = 0.01, Pr = 10$

bottom wall decreases with the increase in Re, but reverse observation is seen next to upper wall. Also, ϕ increases with the augmentation of Re. Figure 4 illustrates the impact of Hartmann number on various profiles. Temperature profile increases with the augmentation of Hartmann number. Also velocity detracts with the augmentation of Ha. Concentration profile improves with the augmentation of Hartmann number. Figure 5 illustrates the

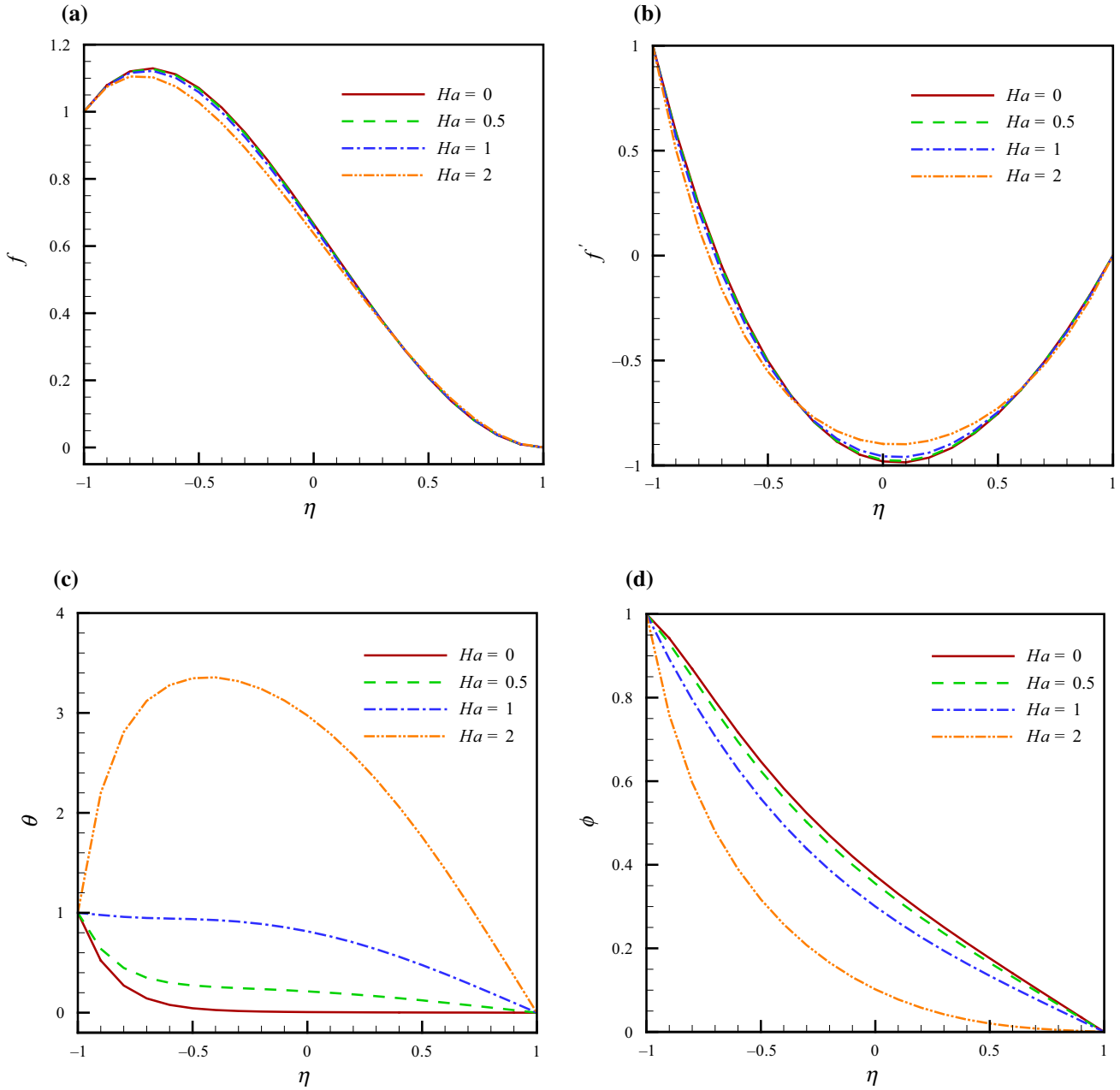

Fig. 4 Effect of Hartman number on velocity, temperature, concentration profiles when $R = 1$, $\lambda = 1, \mathrm{Rd} = 0.5, Ec = 0.5$, $Sc = 1$, $Nt = 0.001, Nb = 0.01, Pr = 10$

roles of suction parameter on various profiles. Temperature and vertical velocity augment with the increase in suction parameter. Horizontal velocity detracts with the augmentation of suction parameter. Also the minimum point of velocity shifts to lower wall. Also concentration has inverse relationship with suction parameter.

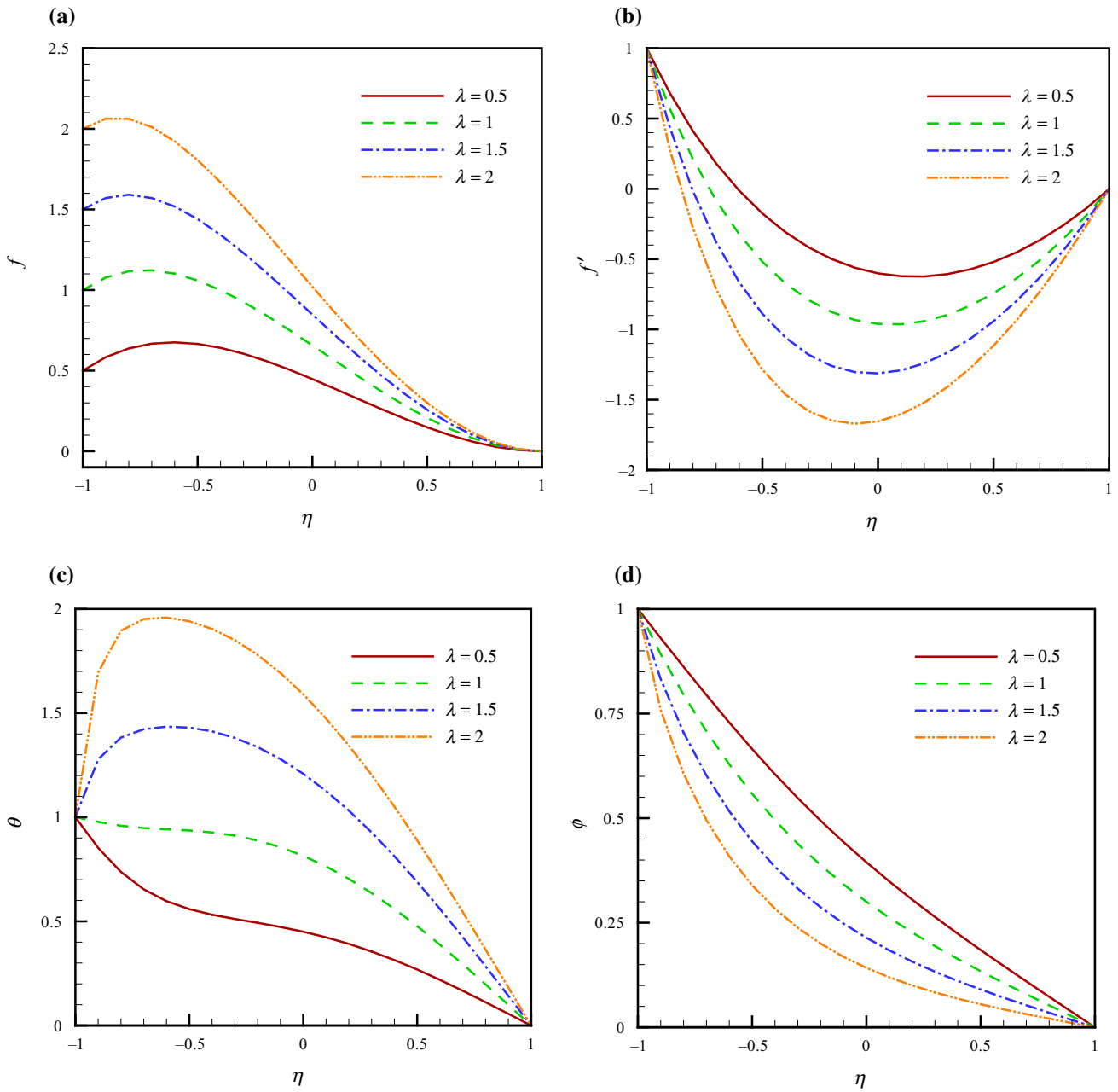

Fig. 5 Effect of suction parameter on velocity, temperature, concentration profiles when $R = 1, Ha = 1, \mathrm{Rd} = 0.5, Ec = 0.5, \ Sc = 1, Nt = 0.001, Nb = 0.01, Pr = 10$

Figure 6 illustrates the roles of radiation on θ profile. θ decreases with the augmentation of Rd. Figure 7 illustrates the impact of Eckert number on θ and ϕ profiles. As Ec augments, the viscous dissipation augments and in turn θ augments with the increase in this parameter. Concentration detracts with the increase in Eckert number. Figure 8

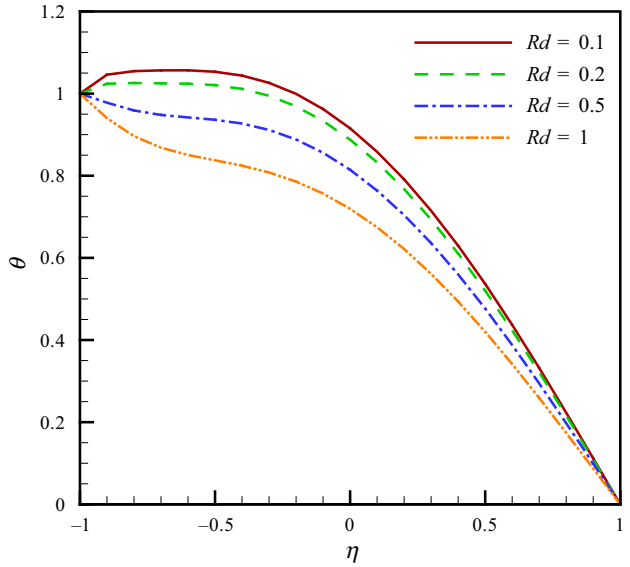

Fig. 6 Effect of radiation parameter on temperature profile when $R = 1, Ha = 1, \lambda = 1, Ec = 0.5, Sc = 1, Nt = 0.001, Nb = 0.01, Pr = 10$

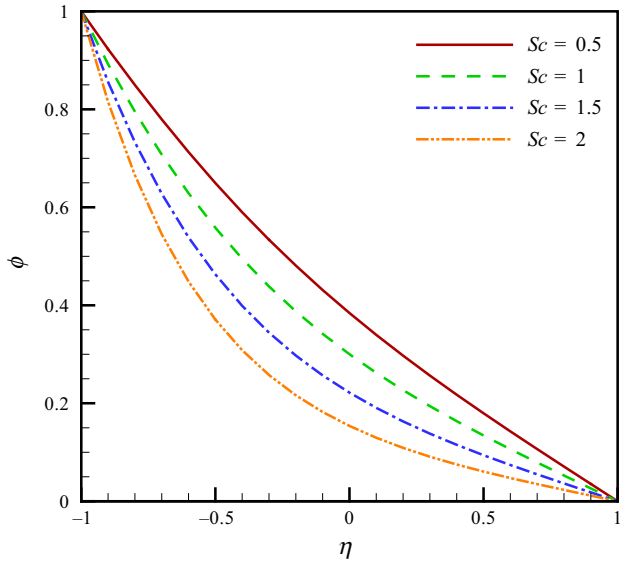

Fig. 8 Effect of Schmidt number on concentration profile when $R = 1, \quad Ha = 1, \lambda = 1, \quad \mathrm{Rd} = 0.5, \quad Ec = 0.5, Nt = 0.001, \quad Nb = 0.01, Pr = 10$

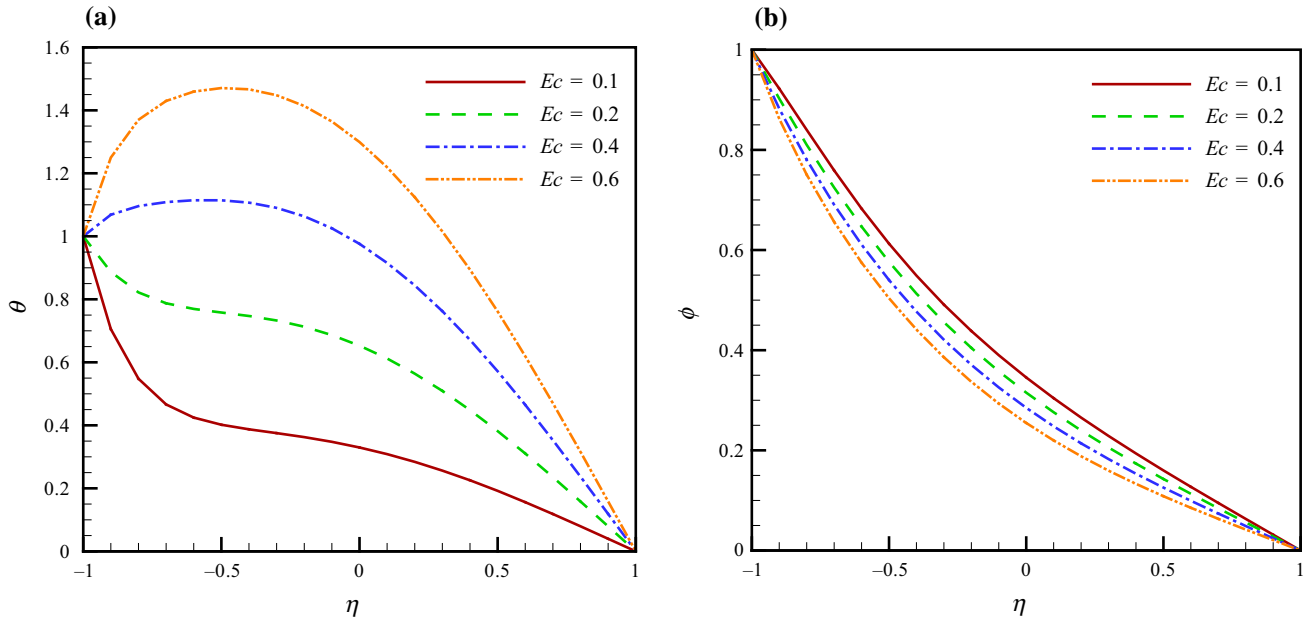

Fig. 7 Effect of Eckert number on temperature and concentration profiles when $R = 1, Ha = 1, \lambda = 1, \mathrm{Rd} = 0.5, Sc = 1, Nt = 0.001, Nb = 0.01, Pr = 10$

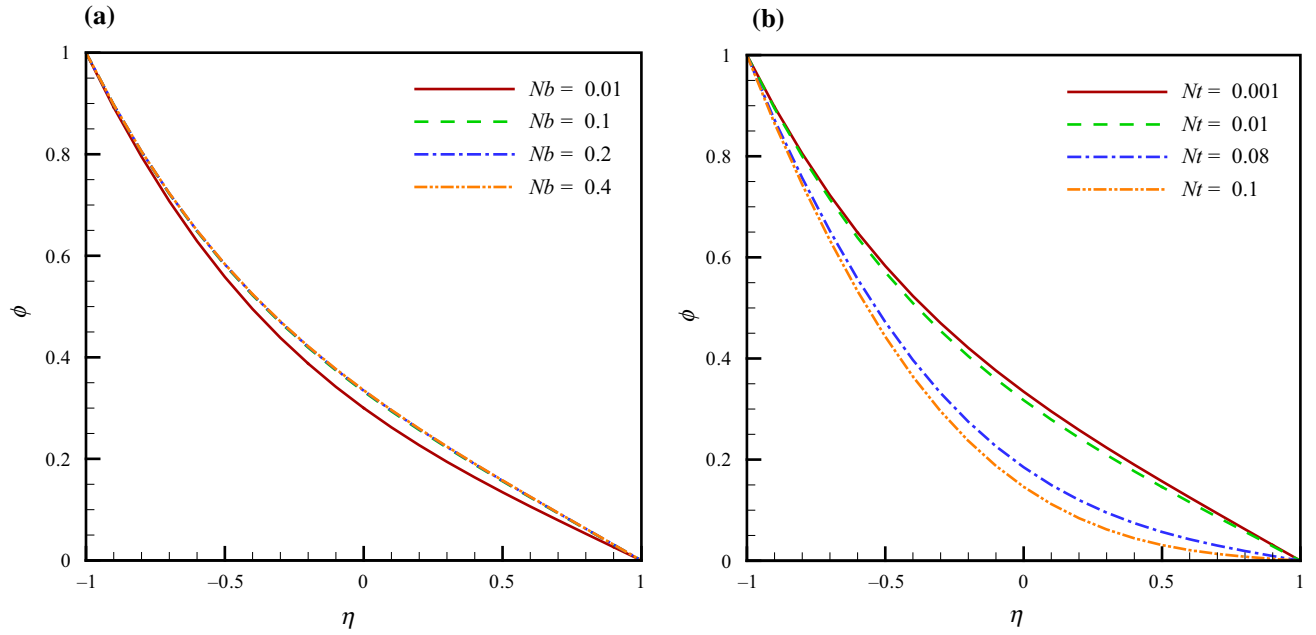

Fig. 9 Effects of Brownian motion parameter and thermophoretic parameter on concentration profile when $R = 1, Ha = 1, \lambda = 1, \mathrm{Rd} = 0.5, Ec = 0.5, Sc = 1, Pr = 10$ **a** $Nt = 0.001$ **b** $Nb = 0.01$

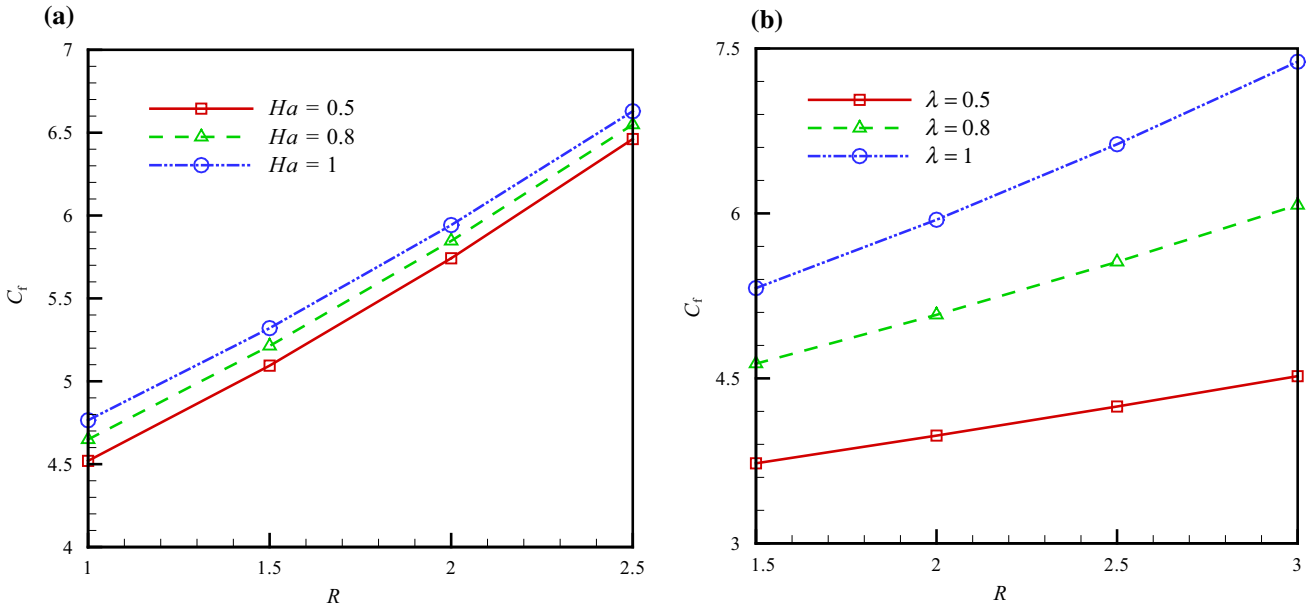

Fig. 10 Effects of suction parameter, Reynolds number, Hartman number on skin friction coefficient **a** $\lambda = 1$ **b** $Ha = 1$

illustrates the impact of Sc on ϕ profile. Increasing Schmidt number causes ϕ to decrease. Figure 9 demonstrates the impacts of Nb and Nt on ϕ profile. ϕ augments with the increase in Nb, while it decreases with the augmentation of Nt. Figure 10 exhibits the influences of suction parameter, Re, and Hartman number on C_f. C_f augments with the

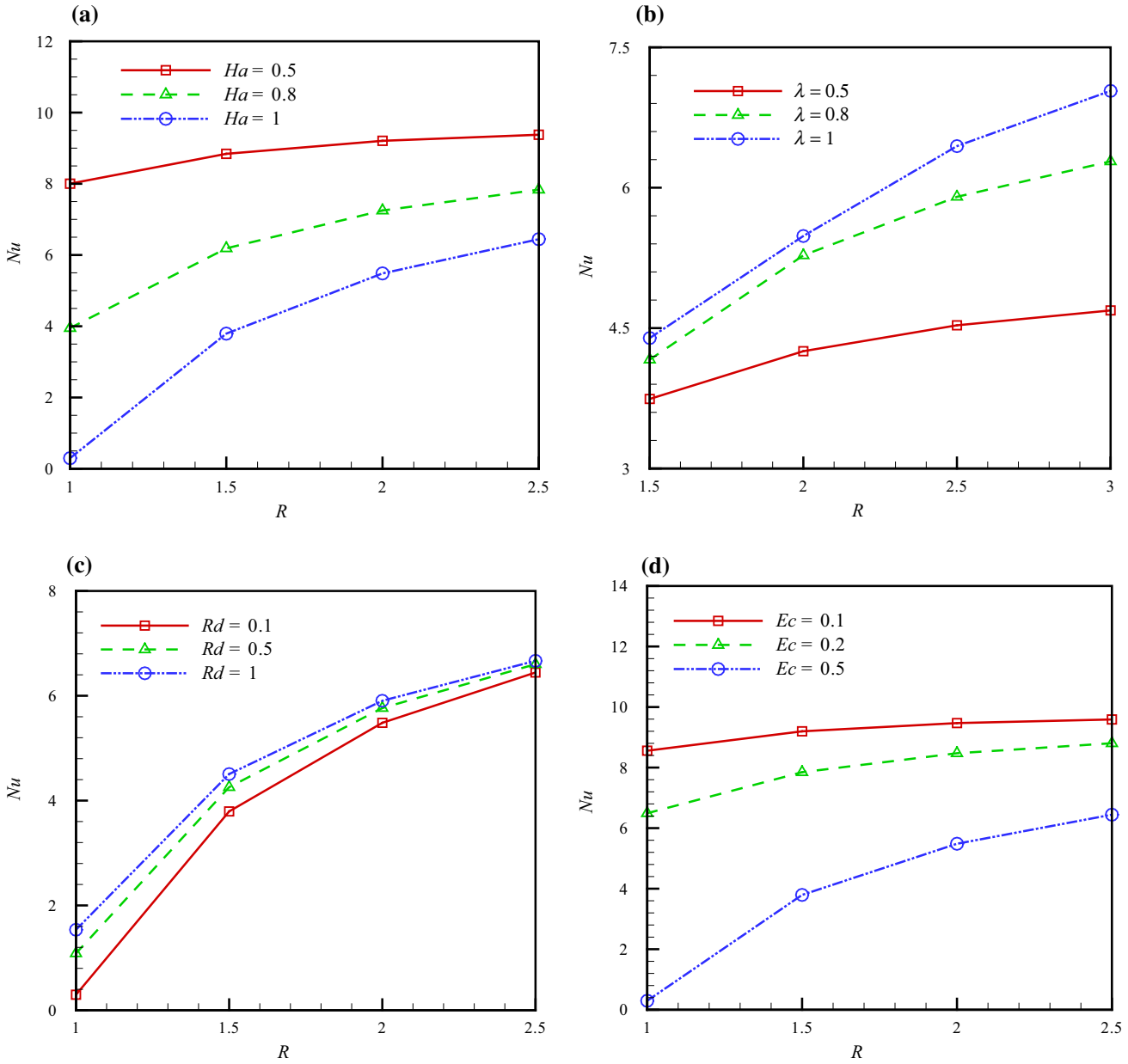

Fig. 11 Effects of Hartmann number, Eckert number, suction parameter, radiation parameter, Reynolds number on Nusselt number when **a** $\lambda = 1, \mathrm{Rd} = 0.5, Ec = 0.5$ **b** $Ha = 1$, $\mathrm{Rd} = 0.5, Ec = 0.5$ **c** $Ha = 1$, $\lambda = 1, Ec = 0.5$ **d** $Ha = 1$, $\lambda = 1, \mathrm{Rd} = 0.5$ $Sc = 1, Nt = 0.001, Nb = 0.01, Pr = 10$

increase in suction parameter, *Re*, and Hartman number. Figure 11 depicts the impact of Hartmann number, Eckert number, suction parameter, Rd, *Re* on *Nu*. Nu augments with the increase in Rd, suction parameter and Re. θ' decreases with the augmentation of Lorentz forces and Eckert number. Tables 1 and 2 depict the influence of Nb and Nt on Nu. Nu detracts with the augmentation of these parameters.

Table 1 Effect of Brownian motion parameter on Nusselt number when $Ha = 1$, $\lambda = 1$,Rd $= 0.5$, $Ec = 0.5$, $Sc = 1$, $Nt = 0.001$, Pr $= 10$

Nu	Nb		
R	0.001	0.04	0.08
1	0.30306	0.275026	0.243478
1.5	3.801208	3.76956	3.733913
2	5.49183	5.458464	5.420864
2.5	6.452456	6.4181	6.379375

Table 2 Effect of thermophoretic parameter on Nusselt number when $Ha = 1$, $\lambda = 1, Rd = 0.5, Ec = 0.5$, $Sc = 1, Nb = 0.2, Pr = 10$

Nu	Nt		
R	0.001	0.05	0.07
1	0.160723	0.117474	0.099823
1.5	3.640233	3.60063	3.584447
2	5.321965	5.28489	5.269732
2.5	6.277456	6.242033	6.227547

Conclusions

Differential transform method is utilized to analyze two-phase nanofluid magnetohydrodynamic flow through a semipermeable duct. Roles of radiation, Brownian motion, suction and thermophoretic parameters, Schmidt number, Hartmann number, Eckert number have been examined. As Hartman number and Eckert number augment, Nu decreases while reverse trend is reported for C_f. Besides it can be reported that Nu improves with increase in Re, Rd and suction parameter but it deceases with the increase in Nb and Nt parameters.

Acknowledgements Authors would like to express their gratitude to King Khalid University, Abha 61413, Saudi Arabia, for providing administrative and technical support.

References

1. Karimipour A, D'Orazio A, Shadloo MS. The effects of different nano particles of Al2O3 and Ag on the MHD nano fluid flow and heat transfer in a microchannel including slip velocity and temperature jump. Physica E. 2017;86:146–53.
2. Maleki H, Safaei MR, Abdullah AA, Alrashed A, Kasaeian A. Flow and heat transfer in non-Newtonian nanofluids over porous surfaces. J Therm Anal Calorim. 2018. https://doi.org/10.1007/s10973-018-7277-9.
3. Sheikholeslami M, Darzi M, Li Z. Experimental investigation for entropy generation and exergy loss of nano-refrigerant condensation process. Int J Heat Mass Transf. 2018;125:1087–95.
4. Hosseini SM, Safaei MR, Goodarzi M, Abdullah AA, Alrashed A, Nguyen TK. New temperature, interfacial shell dependent dimensionless model for thermal conductivity of nanofluids. Int J Heat Mass Transf. 2017;114:207–10.
5. Esfahani JA, Safaei MR, Goharimanesh M, Oliveira LR, Goodarzi M, Shamshirband S, Filho EPB. Comparison of experimental data, modelling and non-linear regression on transport properties of mineral oil based nanofluids. Powder Techno. 2017;317:458–70.
6. Sheikholeslami M, Rokni HB. Simulation of nanofluid heat transfer in presence of magnetic field: a review. Int J Heat Mass Transf. 2017;115:1203–33.
7. Sheikholeslami M, Ganji DD. Nanofluid convective heat transfer using semi analytical and numerical approaches: a review. J Taiwan Inst Chem Eng. 2016;65:43–77.
8. Rizwan UH, Shahzad F, Al-Mdallal QM. MHD pulsatile flow of engine oil based carbon nanotubes between two concentric cylinders. Results Phys. 2017;7:57–68.
9. Sheikholeslami M. Finite element method for PCM solidification in existence of CuO nanoparticles. J Mol Liq. 2018;265:347–55.
10. Arani AAA, AliAkbari O, Safaei MR, Marzban A, Alrashed AAAA, Ahmadi GR, Nguyen TK. Heat transfer improvement of water/single-wall carbon nanotubes (SWCNT) nanofluid in a novel design of a truncated double-layered microchannel heat sink. Int J Heat Mass Transf. 2017;113:780–95.
11. Sheikholeslami M, Jafaryar M, Saleem S, Li Z, Shafee A, Jiang Y. Nanofluid heat transfer augmentation and exergy loss inside a pipe equipped with innovative turbulators. Int J Heat Mass Transf. 2018;126:156–63.
12. Khodabandeh E, Safaei MR, Akbari S, AliAkbari O, Alrashed AAAA. Application of nanofluid to improve the thermal performance of horizontal spiral coil utilized in solar ponds: geometric study. Renew Energy. 2018;122:1–16.
13. Tao YB, He YL. Effects of natural convection on latent heat storage performance of salt in a horizontal concentric tube. Appl Energy. 2015;143(1):38–46.
14. Ahmed N, Adnan, Khan U, Mohyud-Din ST. Unsteady radiative flow of chemically reacting fluid over a convectively heated stretchable surface with cross-diffusion gradients. Int J Therm Sci. 2017;121:182–91.
15. Sheikholeslami M, Ghasemi A, Li Z, Shafee A, Saleem S. Influence of CuO nanoparticles on heat transfer behavior of PCM in solidification process considering radiative source term. Int J Heat Mass Transf. 2018;126:1252–64.
16. Alrashed AAAA, Gharibdousti MS, Goodarzi M, Oliveira LR, Safaei MR, Filho EPB. Effects on thermophysical properties of carbon based nanofluids: experimental data, modelling using regression, ANFIS and ANN. Int J Heat Mass Transf. 2018;125:920–32.
17. Jafaryar M, Sheikholeslami M, Li Z, Moradi R. Nanofluid turbulent flow in a pipe under the effect of twisted tape with alternate axis. J Therm Anal Calorim. 2018. https://doi.org/10.1007/s10973-018-7093-2.
18. Nasiri H, Abdollahzadeh Jamalabadi MY, Sadeghi R, Safaei MR, Nguyen TK, Shadloo MS. A smoothed particle hydrodynamics approach for numerical simulation of nano-fluid flows. J Therm Anal Calorim. 2018. https://doi.org/10.1007/s10973-018-7022-4.
19. Sheikholeslami M. Solidification of NEPCM under the effect of magnetic field in a porous thermal energy storage enclosure using CuO nanoparticles. J Mol Liq. 2018;263:303–15.
20. Goodarzi M, Safaei MR, Vafai K, Ahmadi G. Investigation of nanofluid mixed convection in a shallow cavity using a two-phase mixture model. Int J Therm Sci. 2014;75:204–20.
21. Sheikholeslami M, Shehzad SA, Li Z. Water based nanofluid free convection heat transfer in a three dimensional porous cavity with hot sphere obstacle in existence of Lorenz forces. Int J Heat Mass Transf. 2018;125:375–86.

22. Kandelousi MS. KKL correlation for simulation of nanofluid flow and heat transfer in a permeable channel. Phys Lett A. 2014;378(45):3331–9.
23. Sheikholeslami M, Ganji DD. Nanofluid flow and heat transfer between parallel plates considering Brownian motion using DTM. Comput Methods Appl Mech Engrg. 2015;283:651–63.
24. Sheikholeslami M, Shehzad SA, Abbasi FM, Li Z. Nanofluid flow and forced convection heat transfer due to Lorentz forces in a porous lid driven cubic enclosure with hot obstacle. Comput Methods Appl Mech Eng. 2018;338:491–505.
25. Sheikholeslami M, Jafaryar M, Li Z. Nanofluid turbulent convective flow in a circular duct with helical turbulators considering CuO nanoparticles. Int J Heat Mass Transf. 2018;124:980–9.
26. Sheikholeslami M, Shehzad SA, Li Z. Nanofluid heat transfer intensification in a permeable channel due to magnetic field using Lattice Boltzmann method. Physica B: Condens Matter. 2018;542:51–8.
27. Sheikholeslami M. Numerical simulation for solidification in a LHTESS by means of Nano-enhanced PCM. J Taiwan Inst Chem Eng. 2018;86:25–41.
28. Jafaryar M, Sheikholeslami M, Li Z. CuO-water nanofluid flow and heat transfer in a heat exchanger tube with twisted tape turbulator. Powder Technol. 2018;336:131–43.
29. Safaei MR, Shadloo MS, Goodarzi MS, Hadjadj A, Goshayeshi HR, Afrand M, Kazi SN. A survey on experimental and numerical studies of convection heat transfer of nanofluids inside closed conduits. Adv Mech Eng. 2016;8(10):1–14.
30. Sheikholeslami M. Numerical modeling of Nano enhanced PCM solidification in an enclosure with metallic fin. J Mol Liq. 2018;259:424–38.
31. Sheikholeslami M, Ghasemi A. Solidification heat transfer of nanofluid in existence of thermal radiation by means of FEM. Int J Heat Mass Transf. 2018;123:418–31.
32. Sheikholeslami M, Shehzad SA. CVFEM simulation for nanofluid migration in a porous medium using Darcy model. Int J Heat Mass Transf. 2018;122:1264–71.
33. Sheikholeslami M, Darzi M, Sadoughi MK. Heat transfer improvement and pressure drop during condensation of refrigerant-based nanofluid: an experimental procedure. Int J Heat Mass Transf. 2018;122:643–50.
34. Sheikholeslami M, Rokni HB. CVFEM for effect of Lorentz forces on nanofluid flow in a porous complex shaped enclosure by means of Non-equilibrium model. J Mol Liquids. 2018;254:446–62.
35. Sheikholeslami M. Magnetohydrodynamic nanofluid forced convection in a porous lid driven cubic cavity using Lattice Boltzmann Method. J Mol Liq. 2017;231:555–65.
36. Sheikholeslami M, Bhatti MM. Active method for nanofluid heat transfer enhancement by means of EHD. Int J Heat Mass Transf. 2017;109:115–22.
37. Sheikholeslami M, Shehzad SA. Thermal radiation of ferrofluid in existence of Lorentz forces considering variable viscosity. Int J Heat Mass Transf. 2017;109:82–92.
38. Sheikholeslami M, Rokni HB. Magnetic nanofluid flow and convective heat transfer in a porous cavity considering Brownian motion effects. Phys Fluids. 2018;10(1063/1):5012517.
39. Sheikholeslami M, Shehzad SA. Simulation of water based nanofluid convective flow inside a porous enclosure via Non-equilibrium model. Int J Heat Mass Transf. 2018;120:1200–12.
40. Sheikholeslami M, Seyednezhad M. Simulation of nanofluid flow and natural convection in a porous media under the influence of electric field using CVFEM. Int J Heat Mass Transf. 2018;120:772–81.
41. Sheikholeslami M, Hayat T, Muhammad T, Alsaedi A. MHD forced convection flow of nanofluid in a porous cavity with hot elliptic obstacle by means of Lattice Boltzmann method. Int J Mech Sci. 2018;135:532–40.
42. Sheikholeslami M. Numerical investigation of nanofluid free convection under the influence of electric field in a porous enclosure. J Mol Liq. 2018;249:1212–21.
43. Rashidi MM, Nasiri M, Shadloo MS, Yang Z. Entropy generation in a circular tube heat exchanger using nanofluids: Effects of different modeling approaches. Heat Transf Eng. 2017;38(9):853–66.
44. Shadloo MS, Hadjadj A, Hussain F. Statistical behavior of supersonic turbulent boundary layers with heat transfer at $M\propto = 2$. Int J Heat Fluid Flow. 2015;53:113–34.
45. Sheikholeslami M. CuO-water nanofluid flow due to magnetic field inside a porous media considering Brownian motion. J Mol Liq. 2018;249:921–9.
46. Sheikholeslami M, Rokni HB. Numerical simulation for impact of Coulomb force on nanofluid heat transfer in a porous enclosure in presence of thermal radiation. Int J Heat Mass Transf. 2018;118(2018):823–31.
47. Sheikholeslami M. Numerical investigation for CuO-H2O nanofluid flow in a porous channel with magnetic field using mesoscopic method. J Mol Liq. 2018;249:739–46.
48. Sheikholeslami M, Shehzad SA. Numerical analysis of Fe_3O_4–H_2O nanofluid flow in permeable media under the effect of external magnetic source. Int J Heat Mass Transf. 2018;118:182–92.
49. Sheikholeslami M, Sadoughi MK. Simulation of CuO-water nanofluid heat transfer enhancement in presence of melting surface. Int J Heat Mass Transf. 2018;116:909–19.
50. Sheikholeslami M, Seyednezhad M. Lattice Boltzmann method simulation for CuO-water nanofluid flow in a porous enclosure with hot obstacle. J Mol Liq. 2017;243:249–56.
51. Sheikholeslami M, Hayat T, Alsaedi A. On simulation of nanofluid radiation and natural convection in an enclosure with elliptical cylinders. Int J Heat Mass Transf. 2017;115:981–91.
52. Sheikholeslami M. Influence of magnetic field on nanofluid free convection in an open porous cavity by means of Lattice Boltzmann Method. J Mol Liq. 2017;234:364–74.
53. Goodarzi M, Kherbeet AS, Afrand M, Sadeghinezhad E. Investigation of heat transfer performance and friction factor of a counter-flow double-pipe heat exchanger using nitrogen-doped, graphene-based nanofluids. Int Commun Heat Mass Transf. 2016;76:16–23.
54. Safaei MR, Gooarzi M, Akbari OA, Shadloo MS, Dahari M, Book CH, Performance evaluation of nanofluids in a rib-microchannel for electronics cooling application. In: The book: electronics cooling. InTech Publications; 2016.
55. Sheikholeslami M, Shehzad SA. CVFEM for influence of external magnetic source on Fe_3O_4–H2O nanofluid behavior in a permeable cavity considering shape effect. Int J Heat Mass Transf. 2017;115:180–91.
56. Sheikholeslami M, Seyednezhad M. Nanofluid heat transfer in a permeable enclosure in presence of variable magnetic field by means of CVFEM. Int J Heat Mass Transf. 2017;114:1169–80.
57. Sheikholeslami M, Rokni HB. Melting heat transfer influence on nanofluid flow inside a cavity in existence of magnetic field. Int J Heat Mass Transf. 2017;114:517–26.
58. Sheikholeslami M. Magnetic field influence on CuO -H2O nanofluid convective flow in a permeable cavity considering various shapes for nanoparticles. Int J Hydrogen Energy. 2017;42:19611–21.
59. Sheikholeslami M. Influence of Lorentz forces on nanofluid flow in a porous cavity by means of non-darcy model. Eng Comput. 2017;34(8):2651–67.

60. Sheikholeslami M, Shehzad SA. Magnetohydrodynamic nanofluid convective flow in a porous enclosure by means of LBM. Int J Heat Mass Transf. 2017;113:796–805.
61. Sheikholeslami M, Sadoughi M. Mesoscopic method for MHD nanofluid flow inside a porous cavity considering various shapes of nanoparticles. Int J Heat Mass Transf. 2017;113:106–14.
62. Sheikholeslami M. Lattice Boltzmann method simulation of MHD non-darcy nanofluid free convection. Phys B. 2017;516:55–71.
63. Sheikholeslami M, Bhatti MM. Forced convection of nanofluid in presence of constant magnetic field considering shape effects of nanoparticles. Int J Heat Mass Transf. 2017;111:1039–49.
64. Sheikholeslami M. CuO-water nanofluid free convection in a porous cavity considering Darcy law. Eur Phys J Plus. 2017;132:55. https://doi.org/10.1140/epjp/i2017-11330-3.
65. Sheikholeslami M. Numerical investigation of MHD nanofluid free convective heat transfer in a porous tilted enclosure. Eng Comput. 2017;34(6):1939–55.
66. Sheikholeslami M. Magnetic field influence on nanofluid thermal radiation in a cavity with tilted elliptic inner cylinder. J Mol Liq. 2017;229:137–47.
67. Sheikholeslami M. Numerical simulation of magnetic nanofluid natural convection in porous media. Phys Lett A. 2017;381:494–503.
68. Sheikholeslami M. Influence of Lorentz forces on nanofluid flow in a porous cylinder considering Darcy model. J Mol Liq. 2017;225:903–12.
69. Sheikholeslami M. CVFEM for magnetic nanofluid convective heat transfer in a porous curved enclosure. Eur Phys J Plus. 2016;131:413. https://doi.org/10.1140/epjp/i2016-16413-y.
70. Sheikholeslami M, Rokni HB. Nanofluid two phase model analysis in existence of induced magnetic field. Int J Heat Mass Transf. 2017;107:288–99.
71. Sheikholeslami M, Chamkha AJ. Influence of Lorentz forces on nanofluid forced convection considering Marangoni convection. J Mol Liq. 2017;225:750–7.
72. Sheikholeslami M. Influence of Coulomb forces on Fe_3O_4-H_2O nanofluid thermal improvement. Int J Hydrogen Energy. 2017;42:821–9.
73. Sheikholeslami M, Vajravelu K, Rashidi MM. Forced convection heat transfer in a semi annulus under the influence of a variable magnetic field. Int J Heat Mass Transf. 2016;92:339–48.
74. Sheikholeslami M, Li Z, Shamlooei M. Nanofluid MHD natural convection through a porous complex shaped cavity considering thermal radiation. Phys Lett A. 2018;382:1615–32.
75. Shadloo MS, Hadjadj A. Laminar-turbulent transition in supersonic boundary layers with surface heat transfer: a numerical study. Numer Heat Transf Part A: Appl. 2017. https://doi.org/10.1080/10407782.2017.1353380.
76. Raptis A. Radiation and free convection flow through a porous medium. Int Commun Heat Mass Transf. 1998;25:289–95.
77. Vajravelu K, Kumar BVR. Analytic and numerical solutions of coupled nonlinear system arising in three-dimensional rotating flow. Int J Non-Linear Mech. 2004;39:13–24.
78. Mehmood A, Ali A. Analytic solution of three-dimensional viscous flow and heat transfer over a stretching flat surface by homotopy analysis method. ASME J Heat Trans. 2008;130:12701-1–7.